

## An Optimized Method for PDEs-Based Geometric Modeling and Reconstruction

<sup>1</sup>Chuanjun Wang, <sup>1</sup>Xuefeng Bai, <sup>2</sup>Liyang Yu, <sup>1</sup>Li Li and <sup>1,2</sup>Xiamu Niu

<sup>1</sup>Shenzhen Graduate School, Harbin Institute of Technology, Shenzhen 518055, China

<sup>2</sup>School of Computer Science and Technology, Harbin Institute of Technology,  
Harbin 150080, China

---

**Abstract:** This study presents an optimized method for efficient geometric modeling and reconstruction using Partial Differential Equations (PDEs). Based on the identification between the analytic solution of Bloor Wilson PDE and the Fourier series, we transform the problem of model selection for PDEs-based geometric modeling into the problem of significant frequencies selection from Fourier series. With the significance analysis of the Fourier series, a model selection and an iterative surface fitting algorithm are applied to address the problem of over fitting and under fitting in the PDEs-based geometric modeling and reconstruction. Simulations are conducted on both the computer generated geometric surface and the laser scanned 3D face data. Experiment results show the merits of the proposed method.

**Keywords:** Geometric modeling, model selection, partial differential equations, surface reconstruction

---

### INTRODUCTION

With the advent of efficient and affordable 3D scanning devices, the method to obtain geometry information of the objects using 3D scanner becomes popular. As the captured data are always in the scattered form as point cloud data, they are not suitable for direct operations. We commonly need a surface reconstruction process to represent the surface of objects for practical purpose. Currently, a number of different surface modeling and reconstruction methods have been developed. For example, NURBS splines, radial basis functions and PDEs have been applied to model and reconstruct the surface from scattered point cloud data (Gengoux and Mekhilef, 1993; Carr *et al.*, 2001; Barhak and Fischer, 2001). As the scanned geometric objects are usually in the form of scattered data, it is reasonable to first assume an appropriate geometric model and then optimally fit the model to the objects (Kanatani, 1998). However, it is very difficult to derive an appropriate geometric model from the sampled objects, as inappropriate model will lead to the problem of degeneracy, usually caused by the overfitting or underfitting of the assumed geometric model. In the field surface reconstruction, attentions have gradually been paid on such problems. Ohtake *et al.* proposed an algorithm to penalize overfitting by adding a regularization term to the usual distance error metric between the model and the sample (Ohtake *et al.*, 2004). Steinke *et al.* (2005) used a regularization term

determined with extra-sample validations to avoid overfitting (Steinke *et al.*, 2005). Lee *et al.* proposed a method based on the extra sample validation for the overfitting control in surface reconstruction (Lee *et al.*, 2006).

As an advanced geometric modeling tool, partial differential equations have been widely applied to the objects like 3D face (Sheng *et al.*, 2011), marine propellers (Dekanski *et al.*, 1995), airplane (Bloor and Wilson, 1995), reverse engineering objects (Barhak and Fischer, 2001), etc. In these models, the assumed geometric models are usually empirically selected or directly truncated using a brutal-force threshold from the solution of PDEs. As a result, the reconstructed geometric models are of acceptable visual results, but usually redundant. And the risk of model degeneracy caused by overfitting and underfitting also exist. So far as we know, the overfitting and underfitting problems in the PDEs-based geometric modeling have not yet been discussed. In this study, we proposed an optimized method to infer an appropriate model for the geometric surface modeling and reconstruction using partial differential equations.

### METHODOLOGY

**PDEs-based geometric surface modeling:** In the PDEs-based geometric surface modeling, a piece of surface  $s(u, v) = y(u, v), z(u, v)$  is represented as the solution to an elliptic partial differential equation in a parametric domain, where the parametric domain  $(u, v)$  is derived

from the physical space. The process to reconstruct the shape surface is first to extract the boundary condition curves from the scattered point cloud data and then fit the assumed model to these curves. One of the commonly used PDE is the Bloor Wilson PDE (Bloor and Wilson, 1989; Bloor and Wilson, 1990), and its general form is given by Eq. (1):

$$\left(\frac{\partial^2}{\partial u^2} + a^2 \frac{\partial^2}{\partial v^2}\right) S(u, v) = 0 \quad (1)$$

where,  $S(u, v)$  denotes the surface patch of the reconstructed objects,  $u$  and  $v$  are the parametric surface coordinates derived from the physical space.  $a \leq 1$  is a parameter inherent to the PDE. In order to determine the analytic solution of Eq. (1), four of the boundary condition curves  $B_1, B_2, B_3, B_4$  in Eq. (2) are necessarily needed:

$$\begin{aligned} S(0, v) &= B_1(v) \\ S(s, v) &= B_2(v) \\ S(s, v) &= B_3(v) \\ S(1, v) &= B_4(v) \end{aligned} \quad (2)$$

where,  $B_1(v)$  and  $B_4(v)$  define the edges of the surface at  $u = 0$  and  $u = 1$ , respectively.  $B_2(v)$  and  $B_3(v)$  are the internal second and third curves that restrict the geometric shape at position  $s$  and  $t$ , in which  $0 \leq s < t, s < t \leq 1$ . Figure 1 shows an example of the PDE boundary condition curves and the corresponding surface shapes.

Restricting the boundary conditions to periodic boundary conditions and choosing the parametric region to be  $0 \leq u \leq 1$  and  $0 \leq v \leq 2\pi$ , the parameter value of  $S(u, v)$  can be determined by the specific boundary condition curves. Using the method of separation of variables, the analytic solution of Eq. (1) can be expressed as Eq. (3):

$$S(u, v) = A_0(u) + \sum_{n=1}^{\infty} [A_n(u) \cos(nv) + B_n(u) \sin(nv)] \quad (3)$$

where,

$$\begin{aligned} A_0(u) &= \alpha_{00} + \alpha_{01}u + \alpha_{02}u^2 + \alpha_{03}u^3 \\ A_n(u) &= \alpha_{n1}e^{anu} + \alpha_{n2}ue^{anu} + \alpha_{n3}e^{-anu} + \alpha_{n4}ue^{-anu} \\ B_n(u) &= \beta_{n1}e^{anu} + \beta_{n2}ue^{anu} + \beta_{n3}e^{-anu} + \beta_{n4}ue^{-anu} \end{aligned}$$

Equation (3) is the general form of the analytic solution of Eq. (1). To determine the value of parameters  $\{\alpha_{00}, \alpha_{01}, \alpha_{02}, \alpha_{03}, \alpha_{n1}, \alpha_{n2}, \alpha_{n3}, \alpha_{n4}, \beta_{n1}, \beta_{n2}, \beta_{n3}, \beta_{n4}, n = 1, 2, \dots, K\}$  Fourier analysis are generally applied on the four boundary curves, respectively. In the case that the

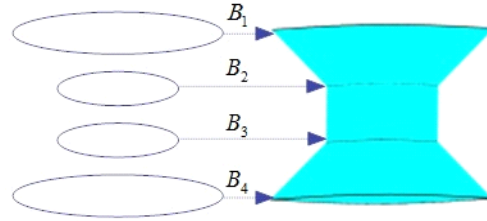


Fig. 1: Example of the boundary curves and corresponding PDE surface

boundary condition curves  $B_1, B_2, B_3, B_4$  can be represented as finite Fourier series, the PDE parameters in Eq. (3) are also finite. However, in the case that  $B_1, B_2, B_3, B_4$  are not expressible as finite Fourier series, approximation methods are needed for practical use. Since the spectral approximation method (Bloor and Wilson, 1996) was proposed, it becomes a popular method in the field of PDEs-based surface modeling and reconstruction (Ugail *et al.*, 1999; Ugail and Wilson, 2003; Elyan and Ugail, 2007). In this method, the first  $K$  terms of Eq. (3) are used to approximate the PDE surface, which means  $n = 1, 2, \dots, K$  in Eq. (3). In this case, the remainder term is defined in Eq. (4):

$$r(u, v) = r_1(u)e^{wu} + r_2(u)e^{-wu} + r_3(u)ue^{wu} + r_4(u)ue^{-wu} \quad (4)$$

where  $w$  is chosen as  $w = a(K+1)$  and  $r_1, r_2, r_3, r_4$  are the functions denoting the difference between the original boundary curves and the reconstructed boundary curves.

These traditional methods (Ugail and Wilson, 2003; Elyan and Ugail, 2007) can produce acceptable visual results. However, as the resulting Fourier series are directly truncated using the first several terms, the question on how to derive an appropriate geometric model for PDE based geometric modeling has not yet been addressed. Literature (Bloor and Wilson, 1996) conclude that a Fourier series mode with 5 is often more than adequate while literature (Ugail and Wilson, 2003; Elyan and Ugail, 2007) comments that a Fourier series mode with 6 is often necessary. Meanwhile, in our experiments, we find that a more compact geometric representation of the reconstructed objects can be obtained with the help of model selection, which provide the potential applications of the PDE based geometric modeling, like recognition, geometric shape analysis, etc.

**Details of the optimized method:** As stated above, lack of model selection procedure is a problem need to be addressed. In this section, we transform the problem of model selection for PDEs-based geometric modeling into

the problem of significant frequencies selection from Fourier series. Given the Fourier series of the boundary condition curves, we first analyze the significance of the corresponding Fourier series frequencies and then derive the assumed geometric surface model with a model selection criterion. After that, an iterative residual fitting algorithm is applied to optimally fit the assumed geometric surface model to the scanned point cloud data.

**Model selection:** In the PDE based geometric modeling, we know that each term of  $A_0(u)$ ,  $A_n(u) \cos(nu)$ ,  $B_n(u) \sin(nu)$ ,  $n = 1, 2, \dots$  in Eq. (3) satisfies the general form of the Bloor Wilson PDE in Eq. (1). So the problem of the model selection for PDE based geometric modeling can be state as:

Given a series of boundary conditions, select a sub set of basis function terms from  $A_0(u)$ ,  $A_n(u) \cos(nv)$ ,  $B_n(u) \sin(nv)$ , in Eq. (3) to describe the shape of the object. In other words, The task of model selection is to estimate the basis function terms of  $A_0(u)$ ,  $A_n(u) \cos(nv)$ ,  $B_n(u) \sin(nv)$ , to describe the geometric shape of the objects.

For each of the boundary condition curves, it can be decomposed into a sum of sine and cosine components of different frequencies as illustrated in Eq. (5):

$$B(v) = a_0 / 2 + \sum_{n=1}^{\infty} (a_n \cos(n\omega) + b_n \sin(n\omega)) \quad (5)$$

Noticing that there exists identification between the analytic solution in Eq. (3) and the Fourier series in Eq. (5), we transform the problem of deriving the appropriate model into the problem of significant frequencies selection from Fourier series.

There are different methods to compute the Fourier series of the boundary condition curves. In the proposed method, the Fast Fourier Transform (FFT) is adopted in the model selection module for computation efficiency, while an iterative fitting method is adopted in the fitting process for the reason of accuracy. Even though Fourier transform and Fourier series are widely used, how to choose the significant frequencies is still not well studied (Chung *et al.*, 2007). In order to choose the frequencies that can help to infer the underlying structure of the PDEs-based geometric models, we first resample  $N$  M-dimensional intermediate samples  $f_1, f_2, \dots, f_N$  as perturbed from its true value  $\hat{f}$  along the boundary condition curves. Each resample  $f_\alpha$  is regarded as one dimensional signal and FFT is applied to compute the Fourier series coefficients. On the resulting Fourier series coefficients set, we define the quantified significance of each term of frequencies as Eq. (6). In Eq. (6),  $g_n(\omega)$  represents the Fourier series coefficients of  $a_0$ ,  $a_n$  and  $b_n$  in Eq. (5), corresponding to the real and imaginary part of frequency  $n$ . The symbol  $\hat{g}_n(\omega)$  is the estimated absolute value of

$g_n(\omega)$  with confidence interval  $1 - \delta$ . The threshold  $T_n$  means that we choose the terms that contribute to the Fourier 'significance' at  $T_n$  level in the resulting Fourier series set, or in other words that we ignore the terms that contribute to the Fourier series with a ratio less than  $T_n$ . The reason that we define the significance of the Fourier series in equation is that the intermediate regions of the boundary curves own a smooth bridge transition between the boundary curves. And the significance of the corresponding frequencies indicates the existence of the corresponding frequencies on the whole surface but not only the corresponding boundary condition curves:

$$\psi(g_n(\omega)) = \left\| \frac{N * \hat{g}_n(\omega)}{\sum_{i=1}^N \sum_{n=1}^N \text{abs}(g_{i,n}(\omega))} \right\| \geq T_n \quad (6)$$

when the significant frequencies of Fourier series in Eq. (6) are chosen, the corresponding terms from  $A_0(u)$ ,  $A_n(u) \cos(nv)$ ,  $B_n(u) \sin(nv)$ , in Eq. (3) are selected as basis functions to form the assumed geometric surface models.

**Iterative residual fitting:** When the selected basis functions are identified, the vector valued parameters of the PDEs-based geometric representation can be determined by the corresponding Fourier coefficients.

Given the boundary condition curves, FFT is generally used to compute the corresponding Fourier coefficients (Bloor and Wilson, 1996; Ugail and Wilson, 2003; Elyan and Ugail, 2007). However, we found that FFT is not suitable for the PDEs-based geometric surface fitting, as it needs a predefined regular grid system for each boundary condition curves, which is difficult to be satisfied. In the optimized method, we proposed to compute the corresponding Fourier coefficients in an iterative manner by solving a linear equation system, like that in literature (Chung *et al.*, 2007).

Given the boundary condition curves, the corresponding Fourier coefficients of each boundary condition curves can be computed by solving the linear regression in Eq. (7):

$$F = Y \begin{pmatrix} a0s \\ ans \\ bns \end{pmatrix} + \varepsilon \quad (7)$$

where  $F$  are the M dimensional resampled vector points on each of the boundary condition:

$$\text{curves. } Y = \begin{pmatrix} \Phi_1(p1) & \Phi_2(p1) & \Phi_3(p1) & \dots & \Phi_k(p1) \\ \Phi_1(p2) & \Phi_2(p2) & \Phi_3(p2) & \dots & \Phi_k(p2) \\ \dots & \dots & \dots & \dots & \dots \\ \Phi_1(pn) & \Phi_2(pn) & \Phi_3(pn) & \dots & \Phi_k(pn) \end{pmatrix}$$

are the design matrix,

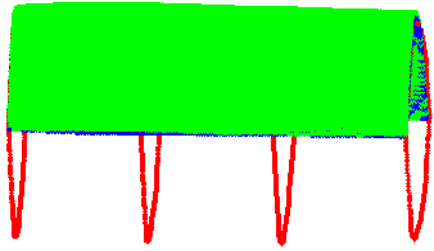


Fig. 2: PDE based geometric modeling and reconstruction. The red line represents the boundary condition curves and the green and blue surface are generated by the traditional and the proposed optimized method, respectively

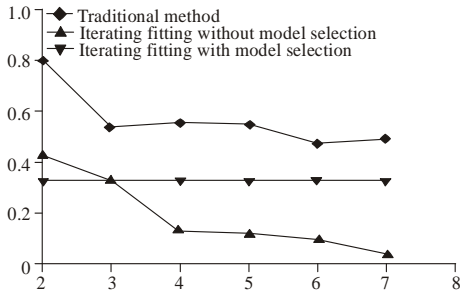


Fig. 3: Comparison of distance errors of different methods. The Fourier series mode is set to 6 in traditional methods.  $Tn\delta$  and  $\delta$  is set to 0.3 and 0.025, respectively in the optimized method

in which  $\{\Phi_i\}_{i=1}^K$  are the selected Fourier frequencies. Iterative residual fitting algorithm (Chung *et al.*, 2007) is then applied on Eq. (7) to compute the corresponding Fourier series coefficients  $a_0s, ans, bns$ .

When the Fourier coefficients of each boundary condition curves are generated, the corresponding PDE parameters can be determined by Eq. (8), (9) and (10), respectively:

$$(\alpha_{00} \alpha_{01} \alpha_{02} \alpha_{03})' = (H_0' H_0)^{-1} H_0 * F_0 \quad (8)$$

$$(\alpha_{n0} \alpha_{n1} \alpha_{n2} \alpha_{n3}) = (H_n' H_n)^{-1} H_n * F_c \quad (9)$$

$$(\beta_{n0} \beta_{n1} \beta_{n2} \beta_{n3}) = (H_n' H_n)^{-1} H_n * F_s \quad (10)$$

where,  $H_0 = \begin{pmatrix} 1 & 0 & 0 & 0 \\ 1 & s & s^2 & s^3 \\ 1 & t & t^2 & t^3 \\ 1 & 1 & 2 & 1 \end{pmatrix}$ ,  $F_0$  are the Fourier series

$$\text{coefficients in Eq. (8). } H_n = \begin{pmatrix} 1 & 0 & 0 & 0 \\ e^{ans} & se^{ans} & e^{-ans} & se^{-ans} \\ e^{ant} & te^{ant} & e^{-ant} & te^{-ant} \\ e^{an} & e^{an} & e^{-an} & e^{-an} \end{pmatrix}, F_c$$

and  $F_s$  are the cosine and sine terms of the Fourier series coefficients in Eq. (9) and (10).

## EXPERIMENTS AND DISCUSSION

There are several merits of the proposed optimized methods. In this section, we first evaluate the accuracy and efficiency improved by the optimized method. Then we investigate the potential abilities of the resulting PDE-based geometric representation for recognition purpose.

**Accuracy and efficiency evaluation:** To evaluate the accuracy and efficiency of the proposed method with model selection, we first use a computer generated geometric shape in our experiments to demonstrate the efficiency of the proposed optimized method. The computer generated geometric surface shape is constructed by the four randomly chosen boundary conditions as:

$$\begin{pmatrix} S(0, v) \\ S(0.33, v) \\ S(0.67, v) \\ S(1, v) \end{pmatrix} = A \begin{pmatrix} \sin(v) \\ \sin(2v) \\ \sin(3v) \\ N(0, 1) \end{pmatrix} \quad (11)$$

$$\text{where, } A = \begin{pmatrix} 20 & 2 & 2 & 0.3 \\ 20 & 3 & 1 & 0.3 \\ 20 & 3 & 2 & 0.3 \\ 20 & 2 & 1 & 0.3 \end{pmatrix}$$

$0 \leq v \leq 2\pi$  and  $N(0, 1)$  is the normal distributed white noise. Figure 2 gives an illustration of the boundary conditions and the corresponding surface representation. For visualization reasons, the range of the reconstructed surface is set to,  $0 \leq v \leq \pi$ . In the simulation, we first resample the 256 scatter points from each of these boundary conditions as the boundary conditions curves, so we get the four boundary conditions in the form of  $4*256$  scatter points. Then, we use these four curves as boundary condition curves to generate the corresponding PDE parameters with different methods. The reconstruction errors is defined as the distance metric introduced by Yang and Medioni (1992) and Lee *et al.* (2006), which measures the point to plane distance between the original points to the reconstructed surface. In Fig. 2, we can see that the optimized method can obtain the similar visual results as the traditional approximation methods. The distance error using different methods are illustrated in Fig. 3. The traditional methods refers to

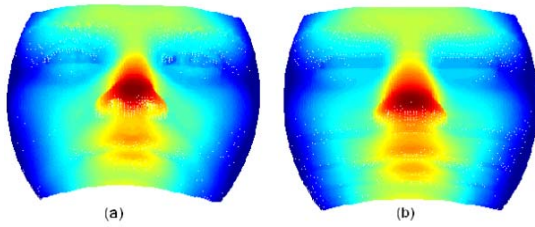


Fig. 4: Visual results of the original and reconstructed 3D face surfaces (a) original 3D face surface (b) reconstructed 3D face surface

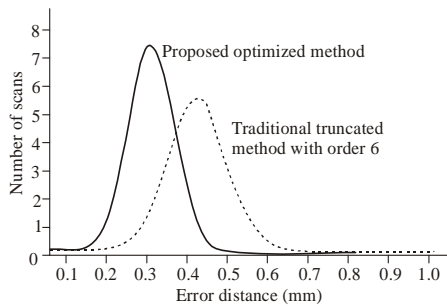


Fig. 5: Demonstration of distance error between the original and the reconstructed 3D face surface

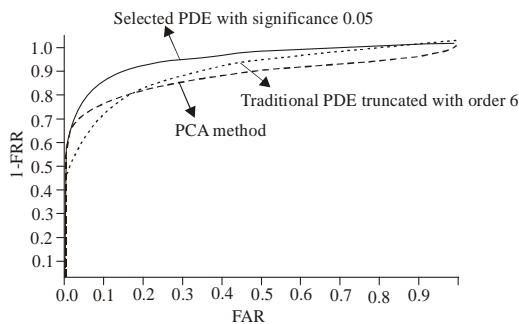


Fig. 6: Comparison of recognition performance between the traditional truncated PDE and the optimized PDE method

the analytic solution of Bloor Wilson PDE resulted from FFT Fourier series (Bloor and Wilson, 1996; Ugail and Wilson, 2003; Elyan and Ugail, 2007), while the other two methods refer to the proposed method with or without model selection. It is obvious that the distance error of traditional truncated methods is much larger than the proposed optimized methods. However, we should not hastily conclude that the smaller the distance error, the better the model, as problem of overfitting might occur. On the iterative fitting methods, when the number of Fourier mode become larger, the distance error seems to decrease in the method without model selection. However, as the noise is 0.3 mm in the experiments, the smaller of the distance error doesn't mean the goodness of

the method but indicate the occurrence of the overfitting. In fact, the geometric model generated by the optimized method with model selection should be the correct one, in which the distance error is a 'stable' value of 0.3584. Specifically on the representation efficiency in the simulation, the number of parameters used to represent the geometric surface can be reduced from  $4 + K*8$  ( $K$  is the order of Fourier series truncated) to  $3*4$ .

We also apply the proposed method on the laser scanned point cloud data for more general applications. We apply the proposed method on the Bosphorus 3D face database (Savran *et al.*, 2008) to model and reconstruct the geometric shapes of the 3D face images from point cloud. The Bosphorus 3D face database features a rich set of expression variations. As there exist pose variations in the scanned 3D face images, we first transform these 3D face into a canonical depth map representation with the methods (Colbry and Stockman, 2009; Wang *et al.*, 2011) After that, the X and Y coordinate of the 3D face images can be regarded as the grid and the depth information Z indicates the shape surface of the 3D face. So, the grid generated by X and Y coordinate can be used to deduce the parametric domain as  $u$  and  $v$ . In order to extend the parametric domain to  $0 \leq u \leq 1$  and  $0 \leq v \leq 2\pi$ , we extend the depth map of the 3D face image with a mirror

$$\text{projection: } SM = \begin{pmatrix} 1 & 0 & 0 \\ 0 & 1 & 0 \\ 0 & 0 & -1 \end{pmatrix} * S$$

in which  $S$  is the original coordinate of  $[X;Y;Z]$ . By this method, the scanned geometric 3D face are extended as  $S = [S \ SM]$ . The parametric domain  $0 \leq u \leq 1$  and  $0 \leq v \leq \pi$  represents the scanned geometric shape of the 3D face while  $0 \leq u \leq 1$  and  $\pi \leq v \leq 2\pi$  represents the extended reflection of the scanned 3D face images. Figure 4 gives the visual results of the original 3D face and the reconstructed geometric surface. Figure 5 demonstrates the distance error between the original surface and the reconstructed representation. As the resolution of the scanner used is 0.4 mm, we can see that the proposed optimized method can get similar results as the traditional methods while the number of the parameters used can be reduced up to 54% for 3D face geometric modeling in our experiment.

**Potential applications:** In many computer vision related applications, efficient and robust representations of the 3D geometric data are necessary. For example, in the face recognition and facial expression analysis applications, it is necessary to robustly and accurately represent the corresponding geometric shape of the objects. (Ugail *et al.*, 2007) have tried to develop a PDE-based 3D face model for biometric application, but the overfitting and underfitting problem were not addressed, which greatly affect the recognition results. In this experiment, we show that the proposed optimized method can help to develop a more efficient and accurate description of the 3D for

such applications with some primary experiment tests. In the experiment, we first normalize the scanned 3D face into a depth map with a size of 256\*256 and then use each four consecutive curves as boundary condition to generate the corresponding PDE representation of the 3D face. Then, we use the Euclidean distance of the resulting PDE parameters to evaluate the performance. Figure 6 gives an illustration of the recognition results. From Fig. 6 we can see that the performance using traditional PDE-based representation is similar to PCA in this database (Alyüz *et al.*, 2008) and when the optimized method is adopted, the performance improves about 10%. It is reasonable because the PDE representation of the optimized method are more robust and the risk of overfitting and underfitting problem are reduced.

### CONCLUSION AND FUTURE WORK

In this study, we address the problem of model selection for PDE-based geometric modeling and reconstruction. Noticing that there exists an identification between the analytic solution of the Bloor Wilson PDEs and the Fourier series of the boundary condition curves, we transform the problem of model selection for the PDE based geometric modeling into the problem of significant frequencies selection from Fourier series. Based on the Fourier analysis of the boundary condition curves, the significance of the Fourier series frequencies is discussed and a model selection criterion is proposed to address the problem of overfitting and underfitting. After that, an iterative fitting algorithm is adopted to generate the parametric representation of the reconstructed geometric objects. Experiments are conducted on both the computer generated surface simulation and the Bosphorus 3D face database. Experiment results show that the proposed optimized method is not only more efficient, but also provide the ability for potential applications. In the future study we plan to go further into the potential applications of the PDE-based geometric representation. Specifically, we will apply the PDE-based 3D face model for facial expression analysis.

### ACKNOWLEDGMENT

This study is supported by the National Natural Science Foundation of China (Project Number: 60832010) and the project of Heilongjiang Department of Education (Project Number: 11551513).

### REFERENCES

Alyüz, N., B. Gkberk, H. Dibekliolu, A. Savran, A. Salah and L. Akarun, 2008. 3D face recognition benchmarks on the Bosphorus database with focus on facial expressions. Biometrics Identity Management workshop (Bio ID), pp: 57-66.

- Barhak, J. and A. Fischer, 2001. Parameterization and reconstruction from 3D scattered points based on neural network and PDE techniques. IEEE T. Vis. Comput. GR, 7: 1-16.
- Bloor, M. and M.J. Wilson, 1989. Generating blend surfaces using partial differential equations. Comput. Aided Design, 21: 165-171.
- Bloor, M. and M.J. Wilson, 1990. Using partial differential equations to generate free-form surfaces. Comput. Aided Design, 22: 202-212.
- Bloor, M. and M.J. Wilson, 1995. Efficient parameterisation of aircraft geometry. J. Aircraft, 32: 1269-1275.
- Bloor, M. and M.J. Wilson, 1996. Spectral approximations to PDE surfaces. Comput. Aided Design, 28: 145-152.
- Carr, J.C., R.K. Beaton, J.B. Cherrie, T.J. Mitchell, W.R. Fright and B.C. McCallum, 2001. Reconstruction and representation of 3D objects with radial basis functions. Proceedings of the ACM SIGGRAPH Conference on Computer Graphics, pp: 67-76.
- Chung, K., K. Dalton, L. Shen, A. Eyans and R. Davidson, 2007. Weighted Fourier series representation and its application to quantifying the amount of gray matter. IEEE T. Med. Imaging, 26(4): 566-581.
- Colbry, D. and G. Stockman, 2009. Real-time identification using a canonical face depth map. IET Comput. Vision, 3: 74-92.
- Dekanski, C.W., M. Bloor and M.J. Wilson, 1995. Generation of propeller blade geometries using the PDE method. J. Ship Res., 39: 108-116.
- Elyan, E. and H. Ugail, 2007. Reconstruction of 3D human facial images using partial differential equations. J. Comput., 2: 1-8.
- Kanatani, K., 1998. Geometric information criterion for model selection. Int. J. Comput. Vision, 26: 171-189.
- Ohtake, Y., A. Belyaev and H.P. Seidel, 2004. 3D scattered data approximation with adaptive compactly supported radial basis functions, Proceedings of Shape Modeling International SMI, pp: 31-39.
- Lee, Y., S. Lee, I. Ivrişimtzis and H.P. Seidel, 2006. Overfitting control for surface reconstruction, Proceedings of Eurographics Symposium on Geometry Processing, Konrad Polthier, Alla Sheffer: Eurographics Association, pp: 231-234.
- Savran, N.A., H. Dibekliolu, O. Eliktutan, B. Gkberk and B. Sankur, 2008. Bosphorus database for 3D face analysis. Lect. Notes Comput. Sc., 5372: 47-56.
- Sheng, Y., P. Willis, G. Castro and H. Ugail, 2011. Facial geometry parameterisation based on partial differential equations. Math. Comput. Model., 54(5): 1536-1548.

- Steinke, F., B. Schlkopf and V. Blanz, 2005. Support Vector Machines for 3D Shape Processing. 3rd Edn, Wiley Online Library, pp: 285-294.
- Ugail, H., M. Bloor and M.J. Wilson, 1999. Techniques for interactive design using the PDE method. *ACM T. Graphic. (TOG)*, 18: 195-212.
- Ugail, H. and M.J. Wilson, 2003. Efficient shape parametrisation for automatic design optimisation using a partial differential equation formulation. *Comput. struct.*, 81: 2601-2609.
- Ugail, H. and E. Elyan, 2007. Efficient 3D data representation for biometric applications, scientific support for the decision making in the security sector. *NATO Science for Peace and Security Series- D: Inf. Commun. Security*, 12: 215-229.
- Wang, X.N., W. Lu and J. Gong, 2011. A hybrid method to build a canonical face depth map. *Int. J. Digital Content Technol. Appl.*, 5: 331-336.
- Yang, C. and G. Medioni, 1992. Object modelling by registration of multiple range images. *Image Vision Comput.*, 10: 145-155.